

Received August 9, 2017, accepted September 13, 2017, date of publication September 18, 2017, date of current version October 12, 2017.

Digital Object Identifier 10.1109/ACCESS.2017.2753459

Time-Averaged Realistic Maximum Power Levels for the Assessment of Radio Frequency Exposure for 5G Radio Base Stations Using Massive MIMO

BJÖRN THORS, ANDERS FURUSKÄR, DAVIDE COLOMBI, AND CHRISTER TÖRNEVIK, (Member, IEEE)

Ericsson Research, SE-16480 Stockholm, Sweden

Corresponding author: Björn Thors (bjorn.thors@ericsson.com)

ABSTRACT In this paper, a model for time-averaged realistic maximum power levels for the assessment of radio frequency (RF) electromagnetic field (EMF) exposure for the fifth generation (5G) radio base stations (RBS) employing massive MIMO is presented. The model is based on a statistical approach and developed to provide a realistic conservative RF exposure assessment for a significant proportion of all possible downlink exposure scenarios (95th percentile) in-line with requirements in a recently developed International Electrotechnical Commission standard for RF EMF exposure assessments of RBS. Factors, such as RBS utilization, time-division duplex, scheduling time, and spatial distribution of users within a cell are considered. The model is presented in terms of a closed-form equation. For an example scenario corresponding to an expected 5G RBS product, the largest realistic maximum power level was found to be less than 15% of the corresponding theoretical maximum. For far-field exposure scenarios, this corresponds to a reduction in RF EMF limit compliance distance with a factor of about 2.6. Results are given for antenna arrays of different sizes and for scenarios with beamforming in both azimuth and elevation.

INDEX TERMS 5G mobile communication, EMF exposure, base stations, RF EMF compliance, massive MIMO, antenna arrays.

I. INTRODUCTION

Radio frequency (RF) electromagnetic field (EMF) compliance assessments are conducted by manufacturers and operators to make sure that radio base station (RBS) equipment comply with relevant regulatory requirements on human exposure before it is placed on the market and installed on site. The purpose with the RF EMF compliance assessments is to define three dimensional volumes, known as compliance boundaries or exclusion zones, outside of which the RF exposure is below the exposure limits. Based on this, the RBS equipment is installed to make sure that the RF exposure in areas accessible to the general public is below the limits. The basic restrictions of RF EMF exposure are specified in terms of specific absorption rate (SAR) or incident power density depending on frequency, where power density is used at higher frequencies due to the smaller penetration depth in human tissue. In the guidelines specified by the International Commission on Non-Ionizing Radiation Protection (ICNIRP), the transition frequency from SAR to power density is at 10 GHz [1]. For practical exposure

assessments, particularly below 10 GHz, ICNIRP also specifies reference levels in terms of electric and magnetic field strengths or plane-wave equivalent power density. The reference levels, derived for maximum coupling conditions, are to be assessed in free space without presence of the exposed individual [1].

Regional and international RF EMF exposure assessment standards for RBS have been developed, see e.g. [2]–[4]. Traditionally, RF EMF exposure assessments are to be conducted for theoretical maximum power configurations. For 2G, 3G, and 4G mobile communication systems, several studies based on large scale measurements in real networks have shown that the actual transmitted power is significantly below the theoretical maximum, see e.g. [5]–[9]. These findings may be attributed to various effects such as discontinuous transmission, traffic variation and advanced power control mechanisms [9].

From an economical and aesthetic point of view it is desirable to re-use existing RBS sites as new mobile communication technologies are introduced to cope with the

requirements of greater capacity, higher data rates, and lower energy consumption in future networks. For site installations, the combined RF EMF exposure is to be assessed. In this case, the conventional conservative approach to base the RF EMF compliance assessments on theoretical maximum power configurations may lead to overly conservative and very large compliance boundaries that may complicate the installation or even make the site unusable. In [10], results from network-based measurements of multi-technology sites were presented, considering combined contribution from 2G, 3G and 4G radio access technologies. The mean and 95th percentile values were found to be 24% and 29% of the theoretical maximum, respectively, which indicates that using the sum of theoretical maximum power levels for RF EMF compliance assessments is overly conservative.

The fifth generation mobile communication systems (5G) are currently being researched and standardized. 5G radio access technologies will be a key enabler for the development of Internet of Things (IoT) and address several application scenarios including large traffic growth and an increasing demand for high-bandwidth connectivity [11]. Advanced antenna technologies such as massive MIMO and beamforming with phased array antennas will play important roles [12], [13]. 5G mobile communication systems will make use of available spectrum in frequency bands from below 3 GHz up to and including millimeter-wave bands. As the frequency is increased, the propagation and diffraction conditions are worsened [14], [15]. The possibility to transmit energy in the desired direction towards the user by one or more well defined beams becomes crucial. This includes mechanisms for cell search, random access, system-information distribution, and mobility management. Thus, a differentiating factor between 5G New Radio (NR) [16] and previous radio access technologies is the ‘beam centric design’ which aims to transmit energy in the directions where it is needed rather than to constantly transmit energy in a wide angular sector. This focusing of energy in different directions will also impact the realistic exposure of 5G RBS products. An exposure assessment of a 5G NR system employing massive MIMO based on the traditional approach would assume that the theoretical maximum power is transmitted in each possible direction for a time-period in the order of minutes, corresponding to the averaging time of the relevant RF exposure limits [1], [17]. This is very unrealistic, if even possible, and would lead to a very conservative compliance boundary consistent with the envelope of all possible array excitations/beams, where each beam is transmitting at the theoretical maximum output power. Factors such as RBS utilization, time-division duplex (TDD), scheduling time, and spatial distribution of served users are then not considered. As such, the conventional approach of using the theoretical maximum power constitutes a scientifically unjustified bottleneck in the roll-out of new 5G networks.

In the international standard IEC 62232:2017 [4], however, it is specified that RF EMF exposure assessments may be conducted for ‘actual maximum’ exposure conditions

corresponding to the 95th percentile of all possible exposure scenarios. In [18] (and included in [4], a power density model to assess downlink EMF exposure from smart antennas was presented. With the assumption that the number of users served by the RBS is known, the model makes use of a statistical approach to define the bearings of the users to obtain a realistic conservative RF exposure in a certain direction.

In the present paper, the approach in [18] is extended to obtain a realistic conservative RF exposure assessment for a significant proportion of all possible downlink exposure scenarios as function of the RBS utilization and considering factors such as TDD, scheduling time, and spatial distribution of served users in azimuth and elevation. The method is developed in Section II and some results for different installation scenarios are given in Section III. A discussion is provided in Section IV and finally some conclusions are drawn in Section V.

II. METHOD

In this paper, the approach towards realistic maximum RF EMF exposure assessments for a 5G array antenna employing massive MIMO is based on modeling the expectation of the statistically conservative fraction of the total power contributing to the EMF exposure within an arbitrary beam, $\hat{P}(n, \rho)$. This expectation, when given as function of the 5G mobile communication system utilization ρ , may be written as

$$E\left(\hat{P}(\rho)\right) = \sum_{n=1}^{n_{\text{conv}}} \hat{P}(n, \rho) \chi(n, \rho), \quad (1)$$

where $\chi(n, \rho)$ denotes the probability that the system at any specific time instant provides service to n users and $\hat{P}(n, \rho) \propto \rho$. The upper limit n_{conv} corresponds to the number of terms needed for convergence.¹ In the following subsections, different factors influencing the constituents of (1) are discussed. The used coordinate system is given in Fig. 1.

With knowledge of $\hat{P}(n, \rho)$, the realistic conservative RF exposure assessment may be carried out using any applicable method, see e.g. [4], [19]. The actual exposure assessment is out of scope for this paper.

A. RBS UTILIZATION RELATED TO THE NUMBER OF SIMULTANEOUS USERS SERVED BY THE SYSTEM AT A SPECIFIC TIME INSTANT

The 5G mobile communication system will provide service to users for which data are assumed to arrive and be served with intensities λ and μ , respectively. Furthermore, the system is described by an M/M/1 queue based on the following assumptions valid for a short time interval Δt [20], [21]:

- The probability that the number of served users within Δt is increased to $n + 1$ is given by $\chi(n \rightarrow n + 1) = \lambda \Delta t + o(\Delta t)$.

¹The number of terms required for the series in (1) to converge, depends on the system utilization. For a low system utilization convergence is obtained with a few terms. For larger system utilization, some tens of terms are required for convergence.

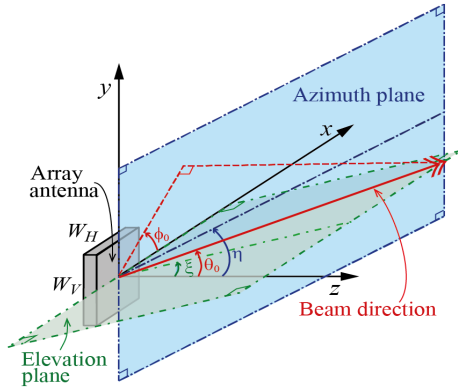


FIGURE 1. Employed coordinate system and definition of azimuth and elevation planes.

- The probability that the number of served users within Δt is decreased to $n - 1$ is given by $\chi(n \rightarrow n - 1) = \mu \Delta t + o(\Delta t)$.
- The arrival and departure of served users are independent processes.
- The probability for more than one arrival or departure is $o(\Delta t)$.
- $\lambda < \mu$ is required to obtain a stable system.

This leads to a set of differential equations which may be solved for a steady state solution to obtain

$$\chi(n, \rho) = \rho^n (1 - \rho), \quad (2)$$

where the system utilization² $\rho = \lambda/\mu$ [20], [21].

B. TIME-DIVISION DUPLEX (TDD)

In TDD, the uplink is separated from the downlink by allocation of different time-slots within the same frequency band. From a downlink exposure assessment point of view, the realistic maximum exposure should be proportional to the fraction of the downlink transmission time to the total time given by

$$F_{TDD} = \frac{DL : UL}{DL : UL + 1}, \quad (3)$$

where $DL : UL$ denotes the downlink/uplink transmission configuration (ratio of downlink transmission time to uplink transmission time).

The downlink/uplink transmission configuration has not yet been standardized for 5G in 3GPP. In Long Term Evolution (LTE), however, seven possible configurations ranging from approximately 2:3 to 9:1 are specified which corresponds to F_{TDD} ranging from about 0.4 to 0.9³ [22], [23]. In this paper, $F_{TDD} = 0.75$ has been assumed as a reasonable value for 5G. For other values of F_{TDD} , the results in Section III may be scaled accordingly.

²The system utilization is defined as the proportion of time that the system is serving one or more connected users.

³Disregarding guard time and time for uplink transmission within the special subframes [22]. This is a conservative assumption from a downlink EMF exposure point of view.

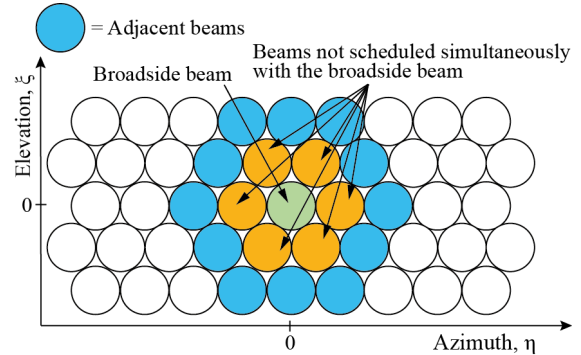


FIGURE 2. Schematic view of different beams to illustrate beamforming in azimuth η and elevation ξ and the employed categorization of the different beams.

C. SPATIAL AND TEMPORAL DISTRIBUTION OF USERS

5G NR array antennas will be designed to allow beamforming in both azimuth and elevation as shown schematically in Fig. 2.

Both a fixed set of beams, using code-book-based precoding, as well as reciprocity based-beamforming will be possible. If the user is located within line-of-sight from the RBS antenna, a focused beam is used. For non-line-of-sight propagation conditions, the system may choose to simultaneously transmit energy in several directions. From an EMF exposure assessment point of view, the maximum exposure is typically obtained when focused beams are used. Therefore, this is the case considered and discussed in this paper.

The assumed spatial distribution of users served by a 5G system will largely impact the obtained results as it influences the probability for how the system directs energy in space. To illustrate the concept, in this paper an expected 5G RBS product designed to cover $\pm 60^\circ$ in azimuth and $\pm 15^\circ$ in elevation is assumed. The approach may easily be generalized to another scan range. Some possible user distribution scenarios (UDS) are illustrated in Fig. 3 in terms of the directional service establishment probability $w(\xi, \eta)$ with the property that its integral over the specified scan range, SR , is unity

$$\iint_{SR} w(\xi, \eta) d\xi d\eta = 1. \quad (4)$$

The directional service establishment probability is the probability that a single user is positioned in the direction (ξ, η) when requiring service. Mathematically, the assumed probabilities may be written as

$$w(\xi, \eta) = \frac{3}{2\pi} \delta(\xi) \quad (\text{Scenario 1}) \quad (5)$$

$$w(\xi, \eta) = \frac{3}{4} \delta(\xi) \cos \frac{3\eta}{2} \quad (\text{Scenario 2}) \quad (6)$$

$$w(\xi, \eta) = \frac{9}{\pi^2} \quad (\text{Scenario 3}) \quad (7)$$

$$w(\xi, \eta) = \frac{9}{\pi} \cos^2 6\xi \cos \frac{3\eta}{2}, \quad (\text{Scenario 4}) \quad (8)$$

where $(\xi, \eta) = (0^\circ, 0^\circ)$ corresponds to the broadside beam direction, see Fig. 2, and δ denotes the Dirac delta function.

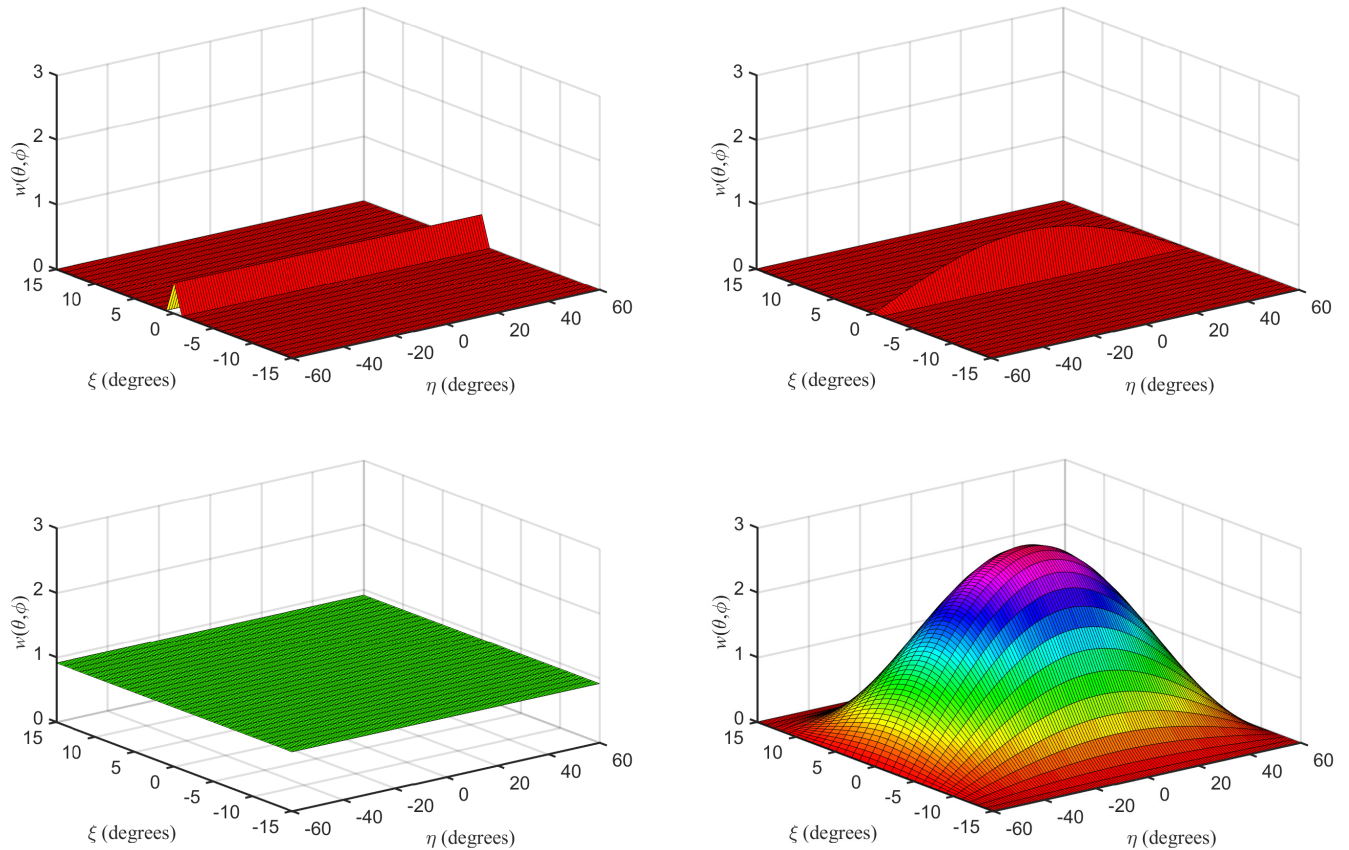


FIGURE 3. Directional service establishment probabilities for different UDS. (a) UDS where the density of users is uniformly distributed in azimuth and no elevation scanning is employed (Scenario 1). This may approximate an RBS installation in a rural environment. (b) UDS where the density of users is weighted by a cosine function in azimuth and no elevation scanning is employed (Scenario 2). This may approximate an RBS installation in a rural environment with a higher density of users in the center of the azimuthal scan range. (c) UDS where the density of users is uniformly distributed in azimuth and elevation (Scenario 3). This may approximate an RBS installation in an urban environment. (d) UDS where the density of users is weighted by a cosine function in azimuth and a squared cosine distribution in elevation (Scenario 4). This may approximate an RBS installation in an urban environment with the highest density of users in the center of both the azimuthal and elevation scan range. The variation in elevation is chosen to reflect a larger density of users in the horizontal plane.

At each time instant, the available power is distributed among the served users. For a far-field scenario, the RF exposure in a certain direction is proportional to the power transmitted in this direction. The service scheduling time in a 5G mobile communication system is normally just a fraction of the time-period corresponding to the RF exposure averaging times specified in [1] and [17]. Since the RF exposure will vary depending on the spatial location of the users, the transmission to all connected users within the averaging time T needs to be considered. A schematic illustration is provided in Fig. 4 showing the beam position and duration of connections as function of scan angle and time for a fictive 5G mobile communication system with 5 different possible beam directions.

With the total average scheduling time per user denoted by T_s , the number of served independent users N during the EMF averaging time T can be approximated in terms of the number of simultaneous users served by the system at a specific time instant, n , by

$$N \approx n \frac{T}{T_s}. \tag{9}$$

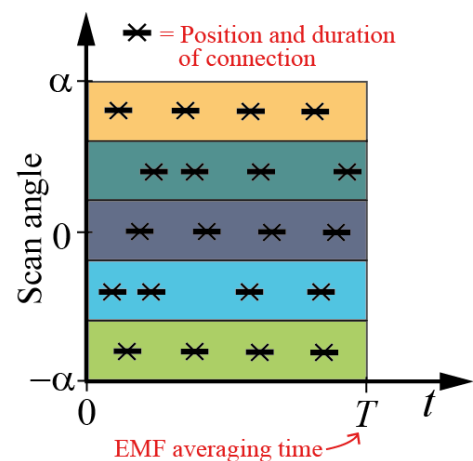


FIGURE 4. Schematic distribution of service connections in a fictive 5G mobile communication system with 5 possible beam directions.

The time ratio T/T_s depends on the system usage pattern. As a realistic conservative approximation $T/T_s \approx 10$, see Appendix. The average number of served users at any time

instant is maintained by an inflow of new users. It is reasonable to assume that the position of a new user within the cell is independent from the position of a previously served user. Thus, to obtain a realistic conservative RF exposure assessment for a significant proportion of all possible downlink exposure scenarios the N independent users are distributed among the available beams according to a relevant UDS, see Fig. 3.

For simplicity, we now focus the description on the broadside beam direction. The approach outlined below, may easily be generalized to any other beam direction. The contributions to the exposure in the broadside beam direction is assumed to consist of three parts [18]:

1. The RF exposure from the broadside beam serving k_{BB} users.
2. The RF exposure from the beams most adjacent to the broadside beam and which serves k_{ADJ} users that may be scheduled simultaneously. The contribution from these sources are weighted with a factor δ_{ADJ} corresponding to the relative contribution from an adjacent beam in the broadside direction. To avoid interference problems, the contribution in the broadside direction from the closest simultaneously scheduled beams is normally suppressed by at least 10 dB, i.e. $\delta_{ADJ} = 0.1$. In this model, this implies that the orange beams in Fig. 2 will not be scheduled simultaneously as the broadside beam and are therefore excluded from the model.
3. The RF exposure from beams outside the adjacent and broadside beam directions that are serving k_{SL} users. The contributions from these sources are weighted with a factor δ_{SL} corresponding to a maximum side lobe level. For a uniformly excited array antenna the maximum side lobe level is about -13.3 dB [24], i.e. $\delta_{SL} = 0.045$.

The number of users in the different beam regions are determined from the inverse of the cumulative binominal distribution functions [18].

$$F_X(k_{BB}) = P(X \leq k_{BB}) = \sum_{i=0}^{k_{BB}} \binom{N}{i} p_{BB}^i (1 - p_{BB})^{N-i} \quad (10)$$

$$\begin{aligned} F_Y(k_{ADJ}) &= P(Y \leq k_{ADJ}) \\ &= \sum_{i=0}^{k_{ADJ}} \binom{N - k_{BB}}{i} p_{ADJ}^i (1 - p_{ADJ})^{N - k_{BB} - i}, \end{aligned} \quad (11)$$

where p_{BB} and p_{ADJ} denote the probabilities that a single user is served by the broadside beam or the adjacent beams, respectively. These probabilities are defined in terms of solid angle ratios weighted with the directional service establishment probability according to

$$p_{BB} = \frac{\Omega_{BBW}(0, 0)}{\sum_{\text{All schedulable beams } i} \Omega_i W(\xi_i, \eta_i)} \quad (12)$$

$$p_{ADJ} = \frac{\sum_{\text{Adjacent beams } j} \Omega_j W(\xi_j, \eta_j)}{\sum_{\text{All schedulable beams } i \text{ except BB}} \Omega_i W(\xi_i, \eta_i)} \quad (13)$$

where the beam solid angle is defined in terms of its half-power beamwidths. For a beam scanned towards (θ_0, ϕ_0) in a spherical coordinate system, the beam solid angle may be approximated by [24]

$$\Omega = \frac{\Theta_H \Theta_V \sec \theta_0}{\sqrt{\sin^2 \phi_0 + \frac{\Theta_H^2}{\Theta_V^2} \cos^2 \phi_0} \sqrt{\sin^2 \phi_0 + \frac{\Theta_V^2}{\Theta_H^2} \cos^2 \phi_0}}, \quad (14)$$

where Θ_H and Θ_V denote the half power beamwidths in the horizontal and vertical planes when scanned towards broadside. These beamwidths are given by [25]

$$\Theta_{H/V} = \frac{0.886\lambda}{W_{H/V}}, \quad (15)$$

where λ and $W_{H/V}$ denotes the wavelength and the array width in the horizontal and vertical planes.

With k_{BB} and k_{ADJ} determined so that the required level of confidence is met, e.g. 95th percentile,

$$k_{SL} = N - k_{BB} - k_{ADJ}. \quad (16)$$

D. FINAL FORM OF THE EXPECTATION OF THE STATISTICALLY CONSERVATIVE FRACTION OF THE TOTAL POWER CONTRIBUTING TO THE EMF EXPOSURE IN THE BROADSIDE BEAM DIRECTION

From the exposition above, the expectation of the statistically conservative fraction of the total power contributing to the EMF exposure in the broadside beam direction can be written as

$$\begin{aligned} E(\hat{P}(\rho)) &= \sum_{n=1}^{n_{\text{conv}}} \frac{\rho T_S}{nT} F_{TDD} \cdot [k_{BB}(n) + k_{ADJ}(n) \delta_{ADJ} \\ &\quad + k_{SL}(n) \delta_{SL}] (1 - \rho) \rho^n \end{aligned} \quad (17)$$

III. RESULTS

Results for the different assumed directional service establishment probabilities in (5) - (8) are given as function of system utilization in Fig. 5 - Fig. 8 assuming a square-shaped array antenna with 8×8 elements and an inter-element distance of half a wavelength. The values of k_{BB} and k_{ADJ} were determined from (10) and (11) to obtain $P(X \leq k_{BB}) \leq 95\%$ and $P(Y \leq k_{ADJ}) \leq 95\%$.

For all investigated UDS and degrees of system utilization, the expectation of the statistically conservative fraction of the total power contributing to the EMF exposure is significantly below the theoretical maximum. The peak value of $E(\hat{P}(\rho))$, obtained for a very large system utilization for the case where the density of users is weighted by a cosine function in azimuth and no elevation scanning is employed, is about 22% of the theoretical maximum power.

Keeping the 0.5λ inter-element distance, in Fig. 9 $\max_{\rho} [E(\hat{P}(\rho))]$ is given as function of array size for square-shaped arrays with $M \times M$ elements for the case that the

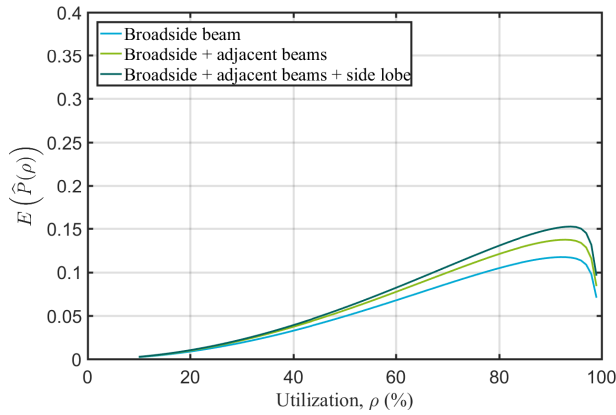


FIGURE 5. Expectation of the statistically conservative fraction of the total power contributing to the EMF exposure when the density of users is uniformly distributed in azimuth and no elevation scanning is employed (Scenario 1).

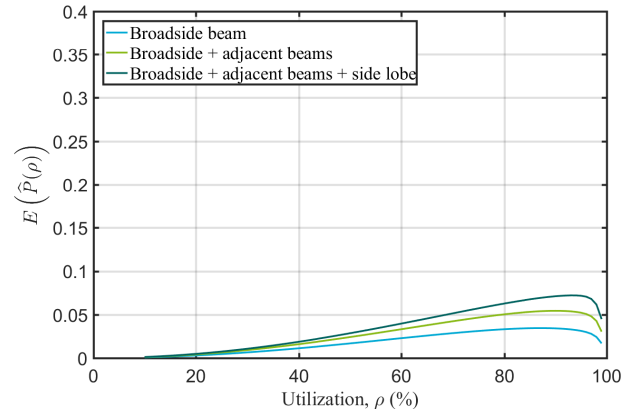


FIGURE 7. Expectation of the statistically conservative fraction of the total power contributing to the EMF exposure when the density of users is uniformly distributed in azimuth and elevation (Scenario 3).

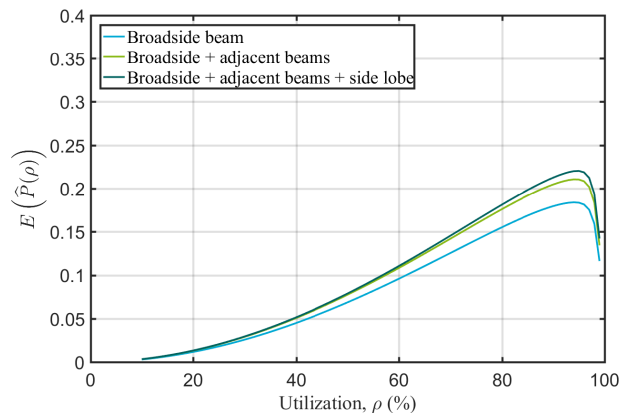


FIGURE 6. Expectation of the statistically conservative fraction of the total power contributing to the EMF exposure when the density of users is weighted by a cosine function in azimuth and no elevation scanning is employed (Scenario 2).

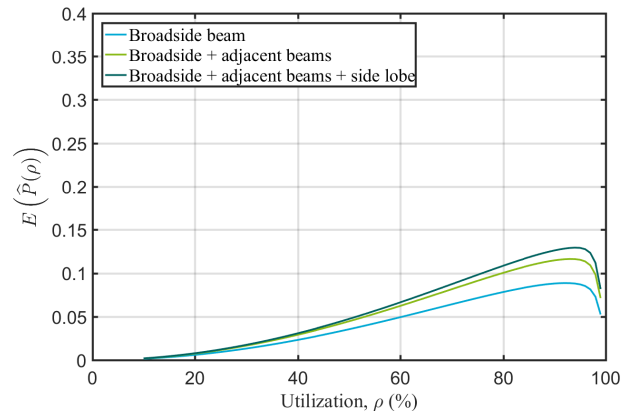


FIGURE 8. Expectation of the statistically conservative fraction of the total power contributing to the EMF exposure when the density of users is weighted by a cosine function in azimuth and a squared cosine distribution in elevation (Scenario 4).

density of users is uniformly distributed in azimuth and no elevation scanning is employed.

As the array size is increased, the solid angles of the beams are reduced. As a consequence, the probabilities in (12) – (13) are reduced which results in a lower $\max_{\rho} [E(\hat{P}(\rho))]$.

IV. DISCUSSION

As mentioned in Section I, an RF EMF exposure assessment of a 5G RBS based on the traditional approach where the theoretical maximum transmit power is allocated to one single user for a time-period of several minutes is very unrealistic. By assuming a total 5G system data rate of 1 Gb/s and an average MP3 song size of 4 MB, it would be possible to download more than 11 000 MP3 songs during a time-period of 6 minutes corresponding to the ICNIRP averaging time for frequencies below 10 GHz [1].

The model in (17) is essentially assuming that the RF EMF exposure is to be assessed in the far-field region of the antenna. To investigate the accuracy of this assumption,

the far-field distance⁴ was compared with the front compliance distance⁵ for a realistic set of power and frequency values. The front compliance distance was calculated using the spherical formula for power density [4] based on the ideal array aperture gain [24] and an RF exposure limit value of 10 W/m² [1]. The obtained results for the considered 8 × 8 array antenna are given in Fig. 10 illustrating that the front compliance distance is larger than the far-field distance for a large part of the considered parameter space which confirms the suitability of the model. This conclusion was found to hold also for the other array sizes considered in Fig. 9.

As stated above, in the IEC 62232:2017 [4] it is specified that RF EMF exposure assessments may be conducted for ‘actual maximum’ exposure conditions corresponding to the 95th percentile of all possible exposure scenarios. From a

⁴Calculated as $2D^2/\lambda$ where D denotes the maximum antenna dimension [26].

⁵The compliance boundary is a surface outside of which the RF EMF exposure is below the exposure limits. The compliance distance is the distance from the antenna to the compliance boundary in a certain direction.

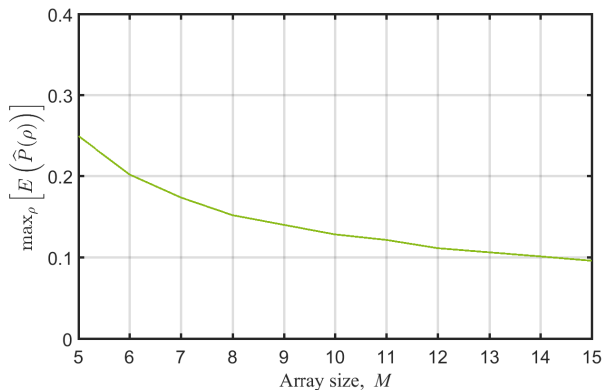


FIGURE 9. Maximum expectation of the statistically conservative fraction of the total power as function of array size when the density of users is uniformly distributed in azimuth and no elevation scanning is employed.

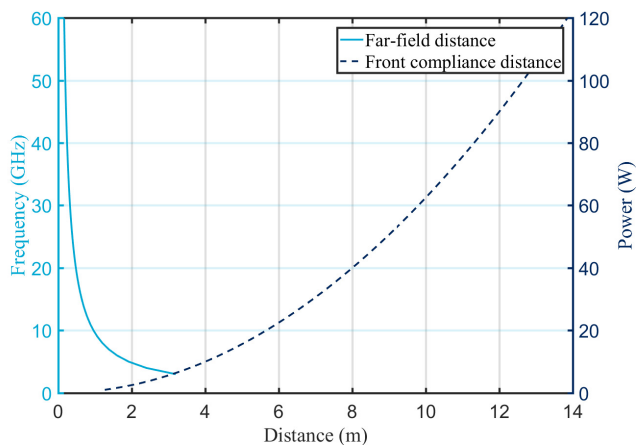


FIGURE 10. Comparison between far-field distance and front compliance distance for the considered 8×8 array.

practical point of view, an interesting question is therefore what the level of confidence in the obtained results would be if an RF exposure assessment were conducted based on the realistic maximum power levels presented above. A quantitative answer to this question would require a careful analysis of a specific 5G RBS product design where the uncertainty in the exposure assessment method is also considered. This is out-of-scope for the present paper but a discussion on the level of conservativeness for the power model in (17) is in place.

The users within the cell were distributed using the cumulative binominal distribution functions to make the exposure contributions from the broadside and adjacent directions conservative for 95% of all possible exposure scenarios. The weight factors δ_{ADJ} and δ_{SL} were chosen to correspond to a realistic upper bound of the contributions from the adjacent beams and the beams contributing via side-lobe exposure. The number of served independent users during the EMF averaging time were chosen to correspond to a realistic maximum activity factor. Thus, this parameter is also chosen conservatively. Finally, as the results are presented in terms of utilization, the level of conservativeness in (16) will also depend on how the utilization is chosen. As expected,

the maximum values for $E(\hat{P}(\rho))$ were found to occur for very large degrees of system utilization. In practice, however, utilization levels close to 100% is unrealistic since this may increase the risk for a reduced quality of service. As a comparison, network-based measurements in a Swedish LTE network conducted during 2016 resulted in a 95th percentile system utilization of about 11% [10]. Based on this, we may conclude that if the level of utilization is not underestimated, the confidence level of (17) is at least 95% and thus may be used in the context of ‘actual maximum exposure conditions’ in IEC 62232:2017 [4].

For Scenario 1, where the density of users is uniformly distributed in azimuth and no elevation scanning is employed, the peak time-averaged realistic maximum power level was found to be about 15% of the theoretical maximum and occur for a system utilization of 94%. This value may be compared with the corresponding long-term⁶ time-averaged value where the available power is evenly distributed among the possible beams. For $F_{TDD} = 0.75$ and $\rho = 0.94$, the long-term time-averaged power level for Scenario 1 is about 8% of the theoretical maximum. The corresponding long-term time-averaged power level for Scenario 3 is 1.5% of the theoretical maximum which may be compared with the peak time-averaged realistic maximum power level of 7% of the theoretical maximum.

In the far-field region, the compliance distance is proportional to the square root of the transmitted power. As an example, a realistic maximum transmitted power of 15% of the theoretical maximum transmitted power corresponds to a reduction in compliance distance of more than 60%.

The next obvious step would be to compare this theoretical model with measurement results. This will be the focus of a follow-up study when 5G networks have been deployed.

V. CONCLUSIONS

In this paper, a theoretical model was presented to estimate the time-averaged realistic maximum power levels for the assessment of RF EMF exposure for 5G Radio Base Stations using Massive MIMO. The model was based on realistic conservative assumptions of a 5G mobile communication system and made use of a statistical approach to distribute the transmitted energy within the cell to obtain results that may be used in context with the ‘actual maximum exposure conditions’ in the international RF EMF exposure assessment standard for radio base stations IEC 62232:2017.

A key parameter of the model is how the users are assumed to be distributed within the cell. For all UDS considered, the time-averaged realistic maximum power levels was found to be significantly below the theoretical maximum. Even for very large degrees of system utilization, the time-averaged realistic maximum was found to take values between 7% - 22% of the theoretical maximum. This translates to reduced compliance distances and may be used to facilitate

⁶The phrase “long-term” is used to denote a sufficiently long time interval to obtain a time-averaged power level corresponding to the considered UDS.

installation of 5G RBS products. The obtained results provide valuable input to standardization of RF EMF exposure assessments in the vicinity of RBS.

APPENDIX

Consider a scenario with a periodic download of web pages, where the web page size is exponentially distributed with a mean page size of 3 MB. This corresponds to a 95th percentile page size of $W_{\text{pagesize}}^{95} = 9$ MB. With an assumed web page load rate of 4 pages per minute, *i.e.* $W_{\text{LR}} = 4/60$ pages per second, and a low peak 5G data rate, $R_{5G} = 50$ Mbit/s = 50/8 MB/s the ratio between the EMF averaging time T and the conservative average scheduling time T_S becomes

$$\frac{T}{T_S} = \frac{R_{5G}}{W_{\text{pagesize}}^{95} W_{\text{LR}}} \approx 10. \quad (18)$$

Another estimation may be conducted based on a streaming media scenario. To obtain high definition (HD) quality using a commercial streaming service a minimum internet connection speed of $R_{\text{Stream,HD}} = 5$ Mbit/s is required [27]. By assuming a low peak 5G data rate of $R_{5G} = 50$ Mbit/s results in an activity factor of 10%, *i.e.* $T/T_S \approx 10$.

REFERENCES

- [1] The International Commission on Non-Ionizing Radiation Protection, "Guidelines for limiting exposure to time-varying electric, magnetic, and electromagnetic fields (up to 300 GHz)," *Health Phys.*, vol. 74, no. 4, pp. 494–522, Apr. 1998.
- [2] *Basic Standard for the Calculation and Measurement of Electromagnetic Field Strength and SAR Related to Human Exposure From Radio Base Stations and Fixed Terminal Stations for Wireless Telecommunication Systems (110 MHz–40 GHz)*, CENELEC Standard EN 50383, CENELEC, Aug. 2010.
- [3] *Product Standard to Demonstrate the Compliances of Radio Base Stations and Fixed Terminal Stations for Wireless Telecommunication Systems With the Basic Restrictions or the Reference Levels Related to Human Exposure to Radio Frequency Electromagnetic Fields (110 MHz–40 GHz)*, CENELEC Standard EN 50385, CENELEC, Jul. 2017.
- [4] *Determination of RF Field Strength and SAR in the Vicinity of Radio Communication Base Stations for the Purpose of Evaluating Human Exposure*, IEC Standard IEC 62232:2017, Aug. 2017.
- [5] Z. Mahfouz, A. Gati, D. Lautru, M.-F. Wong, J. Wiart, and V. F. Hanna, "Influence of traffic variations on exposure to wireless signals in realistic environments," *Bioelectromagnetics*, vol. 33, no. 4, pp. 288–297, 2012.
- [6] D. Colombi et al., "Downlink power distributions for 2G and 3G mobile communication networks," *Radiat. Protection Dosimetry*, vol. 157, no. 4, pp. 477–487, 2013.
- [7] D. Colombi, B. Thors, N. Wirén, L.-E. Larsson, and C. Törnevik, "Measurements of downlink power level distributions in LTE networks," in *Proc. Int. Conf. Electromagn. Adv. Appl. (ICEAA)*, 2013, pp. 98–101.
- [8] A. Bürgi, D. Scanferla, and H. Lehmann, "Time averaged transmitter power and exposure to electromagnetic fields from mobile phone base stations," *Int. J. Environ. Res. Public Health*, vol. 11, no. 8, pp. 8025–8037, 2014.
- [9] P. Joshi, M. Agrawal, B. Thors, D. Colombi, A. Kumar, and C. Törnevik, "Power level distributions of radio base station equipment and user devices in a 3G mobile communication network in India and the impact on assessments of realistic RF EMF exposure," *IEEE Access*, vol. 3, pp. 1051–1059, 2015.
- [10] P. Joshi, B. Thors, D. Colombi, C. Törnevik, and L.-E. Larsson, "Realistic output power levels of multi-technology radio base stations and the implication on RF EMF exposure compliance assessments," in *Proc. Joint Annu. Meet. Bioelectromagn. Soc. Eur. BioElectromagn. Assoc. Co-Org. Eur. COST EMF-MED Action*, paper BM1309, Ghent, Belgium, Jun. 2016, pp. 64–65.
- [11] Ericsson, "5G radio access," Ericsson, Stockholm, Sweden, White Paper 284 23-3204 Uen, Feb. 2016.
- [12] Ericsson, "5G systems," Ericsson, Stockholm, Sweden, White Paper 284 23-3251 Uen, Jan. 2017.
- [13] T. L. Marzetta, "Massive MIMO: An introduction," *Bell Labs Tech. J.*, vol. 20, pp. 11–22, Mar. 2015.
- [14] T. S. Rappaport et al., "Millimeter wave mobile communications for 5G cellular: It will work!" *IEEE Access*, vol. 1, pp. 335–349, 2013.
- [15] S. Deng, G. R. MacCartney, and T. S. Rappaport, "Indoor and outdoor 5G diffraction measurements and models at 10, 20, and 26 GHz," in *Proc. IEEE Global Commun. Conf. (GLOBECOM)*, Dec. 2016, pp. 1–7.
- [16] E. Dahlman et al., "5G wireless access: Requirements and realization," *IEEE Commun. Mag.*, vol. 52, no. 12, pp. 42–47, Dec. 2014.
- [17] *Radiofrequency Radiation Exposure Limits*, Part 1.1310, Code of Federal Regulations CFR title 47, Federal Communications Commission (FCC), Aug. 1997.
- [18] M. Wenhua, M. Huaxing, and G. Peng, "The EMF radiation calculation and measurement for smart antenna," in *Proc. 6th Int. Wireless Commun. Mobile Comput. Conf. (IWCMC)*, 2010, pp. 119–123.
- [19] E. Degirmenci, B. Thors, and C. Törnevik, "Assessment of compliance with RF EMF exposure limits: Approximate methods for radio base station products utilizing array antennas with beam-forming capabilities," *IEEE Trans. Electromagn. Compat.*, vol. 58, no. 4, pp. 1110–1117, Aug. 2016.
- [20] K. S. Trivedi, *Probability and Statistics With Reliability, Queuing, and Computer Science Applications*. Englewood Cliffs, NJ, USA: Prentice-Hall, 1982.
- [21] U. Körner, *Tillförlitlighetsteori och Köteori Applicerat på Telekommunikations- och Datorsystem*, (in Swedish). Studentlitteratur, 1990.
- [22] E. Dahlman, S. Parkvall, J. Sköld, and P. Beming, *3G Evolution: HSPA and LTE for Mobile Broadband*, 2nd ed. New York, NY, USA: Academic, 2008.
- [23] *3rd Generation Partnership Project; Technical Specification Group Radio Access Network; Evolved Universal Terrestrial Radio Access (E-UTRA); Physical Channels and Modulation (Release 14)*, document 3GPP TS 36.211 V14.2.0, 3GPP, Jun. 2017.
- [24] C. A. Balanis, *Antenna Theory: Analysis and Design*. New York, NY, USA: Wiley, 1982.
- [25] R. Elliott, "Beamwidth and directivity of large scanning arrays—First of two parts," *Microw. J.*, pp. 53–60, Dec. 1963.
- [26] *IEEE Standard Definition of Terms for Antennas*, IEEE Standard 145-1993, Antenna Standards Committee of the IEEE Antennas and Propagation Society, Mar. 1993.
- [27] Netflix. *Streaming Netflix in HD*. Accessed Nov. 22, 2017. [Online]. Available: <https://help.netflix.com/en/node/13844>



BJÖRN THORS received the M.Sc. degree in engineering physics from Uppsala University, Sweden, in 1996, and the Ph.D. degree in electromagnetic theory from the Royal Institute of Technology (KTH), Stockholm, Sweden, in 2003.

From 2003 to 2005, he was a Research Associate with KTH. Since 2005, he has been with Ericsson Research, where he is currently a Senior Specialist, working with research and standardization related to radio frequency exposure assessment of wireless equipment.



ANDERS FURUSKÄR received the M.Sc. degree in electrical engineering and the Ph.D. degree in radio communications systems from the Royal Institute of Technology, Stockholm, Sweden, in 1996 and 2003, respectively. He joined Ericsson Research in 1997 and is currently a Senior Expert, focusing on radio resource management and the performance evaluation of wireless networks.



DAVIDE COLOMBI received the M.Sc. (*summa cum laude*) degree in telecommunication engineering from the Politecnico di Milano, Italy, in 2009. Since 2009, he has been with Ericsson Research, Stockholm, Sweden, working with research and standardization related to radio frequency exposure from wireless communication equipment. Since 2014, he has been involved in activities related to EMF compliance of 5G wireless equipment. He is currently a Convener of IEC

TC106 AHG 10 and the Deputy Chair of the EMF standardization working group within the Mobile and Wireless Forum.



CHRISTER TÖRNEVIK (M'98) received the M.Sc. degree in applied physics from Linköping University, Linköping, Sweden, in 1986, and the Lic. (Tech.) degree in materials science from the Royal Institute of Technology, Stockholm, Sweden, in 1991. He joined Ericsson in 1991, and since 1993, he has been involved in research activities related to radio frequency exposure from wireless communication equipment. He is currently a Senior Expert within Ericsson Research and is

responsible for electromagnetic fields and health within the Ericsson Group. From 2003 to 2005, he was the Chairman of the Board of the Mobile Manufacturers Forum, and he is currently the Secretary of the Board. Since 2006, he has been the Chairman of the Technical Committee on Electromagnetic Fields within the Swedish Electrotechnical Standardization Organization, SEK, and he has as an expert contributed to the development of several CENELEC, IEC, and IEEE standards on the assessment of RF exposure from wireless equipment.

• • •